EBioMedicine 71 (2021) 103530

Contents lists available at ScienceDirect

EBioMedicine

journal homepage: www.elsevier.com/locate/ebiom

Identification of a wide spectrum of ciliary gene mutations in nonsyndromic biliary atresia patients implicates ciliary dysfunction as a novel disease mechanism

Wai-Yee Lam[a,b], Clara Sze-Man Tang[a,b], Man-Ting So[a], Haibing Yue[a], Jacob Shujui Hsu[c], Patrick Ho-Yu Chung[a], John M. Nicholls[d], Fanny Yeung[a], Chun-Wai Davy Lee[e], Diem Ngoc Ngo[f], Pham Anh Hoa Nguyen[f], Hannah M. Mitchison[g], Dagan Jenkins[g], Christopher O'Callaghan[h], Maria-Mercè Garcia-Barceló[a], So-Lun Lee[i], Pak-Chung Sham[c], Vincent Chi-Hang Lui[a,b,*], Paul Kwong-Hang Tam[a,b,*]

[a] Division of Paediatric Surgery, Department of Surgery, Li Ka Shing Faculty of Medicine, The University of Hong Kong, LKS Faculty of Medicine Building, 21 Sassoon Road, Hong Kong SAR, China
[b] Dr Li Dak-Sum Research Centre, The University of Hong Kong, Hong Kong SAR, China
[c] Department of Psychiatry, Li Ka Shing Faculty of Medicine, The University of Hong Kong, Hong Kong SAR, China
[d] Department of Pathology, Li Ka Shing Faculty of Medicine, The University of Hong Kong, Hong Kong SAR, China
[e] Department of Paediatrics and Adolescent Medicine, Li Ka Shing Faculty of Medicine, The University of Hong Kong, Hong Kong SAR, China
[f] National Hospital of Pediatrics, Vietnam
[g] Genetics and Genomic Medicine, UCL Great Ormond Street Institute of Child Health, University College London, London, United Kingdom
[h] Respiratory, Critical Care & Anaesthesia Section, UCL Great Ormond Street Institute of Child Health, University College London, London, United Kingdom
[i] Department of Paediatrics and Adolescent Medicine, Queen Mary Hospital, Hong Kong SAR, China

ARTICLE INFO

Article History:
Received 18 January 2021
Revised 9 July 2021
Accepted 27 July 2021
Available online xxx

Keywords:
Biliary atresia
Whole exome sequencing
Rare variants
Cilia dysfunction

ABSTRACT

Background: Biliary atresia (BA) is the most common obstructive cholangiopathy in neonates, often progressing to end-stage cirrhosis. BA pathogenesis is believed to be multifactorial, but the genetic contribution, especially for nonsyndromic BA (common form: > 85%) remains poorly defined.
Methods: We conducted whole exome sequencing on 89 nonsyndromic BA trios to identify rare variants contributing to BA etiology. Functional evaluation using patients' liver biopsies, human cell and zebrafish models were performed. Clinical impact on respiratory system was assessed with clinical evaluation, nasal nitric oxide (nNO), high speed video analysis and transmission electron microscopy.
Findings: We detected rare, deleterious *de novo* or biallelic variants in liver-expressed ciliary genes in 31.5% (28/89) of the BA patients. Burden test revealed 2.6-fold (odds ratio (OR) [95% confidence intervals (CI)]= 2.58 [1.15–6.07], adjusted $p = 0.034$) over-representation of rare, deleterious mutations in liver-expressed ciliary gene set in patients compared to controls. Functional analyses further demonstrated absence of cilia in the BA livers with *KIF3B* and *TTC17* mutations, and knockdown of *PCNT, KIF3B* and *TTC17* in human control fibroblasts and cholangiocytes resulted in reduced number of cilia. Additionally, CRISPR/Cas9-engineered zebrafish knockouts of *KIF3B, PCNT* and *TTC17* displayed reduced biliary flow. Abnormally low level of nNO was detected in 80% (8/10) of BA patients carrying deleterious ciliary mutations, implicating the intrinsic ciliary defects.
Interpretation: Our findings support strong genetic susceptibility for nonsyndromic BA. Ciliary gene mutations leading to cholangiocyte cilia malformation and dysfunction could be a key biological mechanism in BA pathogenesis.
Funding: The study is supported by General Research Fund, HMRF Commissioned Paediatric Research at HKCH and Li Ka Shing Faculty of Medicine Enhanced New Staff Start-up Fund.

* Corresponding authors at: Division of Paediatric Surgery, Department of Surgery, The University of Hong Kong, LKS Faculty of Medicine Building, 21 Sassoon Road, Hong Kong.
E-mail addresses: vchlui@hku.hk (V.C.-H. Lui), paultam@hku.hk (P.K.-H. Tam).

https://doi.org/10.1016/j.ebiom.2021.103530

Research in context

Evidence before this study

Biliary atresia (BA) is a rare, complex hepatobiliary disorder that usually presents during the first few weeks of life. Surgery is the only treatment, yet the outcome is notoriously poor, with less than 60% of patients having long term survival with native liver. Genetics and gene expression studies suggested that the genetic vulnerability of the patient is critical for BA development; however, the genetic etiology of BA remains largely unexplored. Thus far, only one single gene has been linked to syndromic form of BA while a few common variants were associated with increased risk of nonsyndromic BA.

Added value of this study

Using trio-based whole exome sequencing, this study for the first time demonstrated rare variant contribution to nonsyndromic BA, such that rare, *de novo* or biallelic deleterious variants in liver-expressed ciliary genes was associated with a significant two-fold increased risk of BA. This finding suggests that deleterious ciliary mutations may underlie the cholangiocyte cilia abnormalities observed in livers of nonsyndromic BA patients. Depletion of candidate ciliary genes can induce BA-like phenotype of reduced bile flow in zebrafish models, implying that ciliary malformation and dysfunction could be a novel disease mechanism of BA. The low nasal nitric oxide levels detected in most of the BA patients carrying ciliary mutations suggests a genetic predisposition to multisystem ciliary abnormalities.

Implication of all the available evidence

This study provides novel evidence that genetic factors play a major role in a substantial proportion of nonsyndromic BA cases, and a strong genetic basis for the previously reported cholangiocyte ciliary abnormalities. Rare deleterious ciliary mutations predisposed to higher risk of nonsyndromic BA. The predisposition to ciliary dysfunction may act beyond the hepatobiliary system and genetic screening for deleterious mutations in the cilia gene set would allow patient stratification to further assess the pleiotropic clinical features and to improve clinical management. As reflected by the high genetic heterogeneity of ciliary mutations uncovered in this study, the nonsyndromic BA is unlikely to have a single genetic etiology. Patient stratification aided by transcriptomic and immune profiling may help leverage statistical power and elucidate the polygenic etiology of BA.

1. Introduction

Biliary Atresia (BA) is a major cause of neonatal cholestasis, characterized by progressive fibrosclerosing and inflammatory obliteration of the biliary system during the first few weeks of life. BA is rare and varies widely in incidence among populations, being most common in East Asia (1 in 5000 live births in Asians, compared to 1 in 18,000 live births in Caucasians) [1]. The occurrence of BA is mostly sporadic, though a limited number of familial cases have been reported previously [2]. The only current treatment is the Kasai portoenterostomy to restore bile flow. Yet a high proportion of patients, even when bile flow is reestablished, still develop progressive inflammation and sclerosis in the intrahepatic biliary tree, leading to secondary liver cirrhosis. For these patients and those with failed portoenterostomy, liver transplantation is the only treatment option. In neonates, BA is the most common indication for liver transplantation.

BA can be classified into two major groups. The syndromic form, found in 5–20% of BA cases, is characterized by the coexistence of other major congenital anomalies, most commonly laterality defects and splenic malformation. This could be attributed to defective morphogenesis of the bile duct during embryonic development and chromosomal anomalies are a possible genetic origin [3,4]. The nonsyndromic form of BA accounts for over 80% of cases, often presenting with later onset of pale stools and jaundice compared to the syndromic form. Nonsyndromic BA is thought to be caused by a combination of environmental insults and genetic predisposition [5]. It is hypothesized that a still unknown exogenous factor, possibly viral infection (e.g. cytomegalovirus) or toxins (e.g. biliatresone), meets the innate immune system of a genetically predisposed individual and thereby induces an uncontrollable and potentially self-limiting immune response, which manifests as liver fibrosis and atresia of the bile ducts [6,7]. To explore the genetic contribution to BA, we conducted the first genome-wide association studies on nonsyndromic BA and identified *ADD3* as a susceptibility gene, showing that common genetic variants could alter disease risk by affecting *ADD3* expression levels in liver [8,9]. Since then, there has been growing evidence that common genetic variations contribute to BA risk, with the identification of the additional susceptibility loci *GPC* [10], *EFEMP1* [11] and *ARF6* [12]. Recent whole exome sequencing (WES) study on syndromic patients with biliary atresia splenic malformation (BASM) uncovered potentially damaging rare variants in polycystic kidney disease 1 like 1 (*PKD1L1*) involved in laterality determination and ciliary function, which might account for the syndromic presentation of BASM [13]. Yet, convincing evidence that genetic factors act beyond common variant genetic susceptibility in the pathogenesis of nonsyndromic BA remains to be found [14].

We hypothesized that rare coding variants predispose not only to syndromic but also to nonsyndromic BA. Here, we report a trio-based WES study on 89 BA trios (affected proband and unaffected parents), which utilizes the inheritance models to discover a set of liver-expressed ciliary genes enriched with rare, deleterious *de novo* or biallelic mutations in nonsyndromic BA patients. Through functional characterization of candidate ciliary genes in patients' liver biopsies, human cholangiocytes and fibroblast cells as well as zebrafish models, we demonstrated their functional impact on ciliary abnormalities and their relevance to BA phenotype. Lastly, we assessed their clinical impact on patients carrying the rare deleterious mutations with nasal nitric oxide (nNO) test, respiratory evaluation, high speed video analysis and transmission electron microscopy (TEM).

2. Methods

2.1. Human subjects

A total of 91 unrelated nonsyndromic BA patients and their unaffected parents from the Southeast Asian population participated in the study, of which 45 trios were recruited from Queen Mary Hospital, Hong Kong and 46 trios from the National Hospital of Pediatrics in Vietnam. BA was diagnosed by hepatobiliary scintigraphy and operative cholangiography. After sequencing, we excluded two BA trios due to problematic biological relatedness and sample contamination, which resulted in 89 trios for subsequent genetic analysis. Of these 89 BA patients analyzed, 38.2% of the subjects (n = 34) were male and 88.8% (n = 79) had undergone Kasai hepatoportoenterostomy at the average age of 2.2 months (range: 1–7 months).

2.2. Ethics

The study protocol was approved by the Institutional Review Board of the University of Hong Kong - Hospital Authority Hong Kong West Cluster (UW 05–282 T/945). Informed consent, or informed parental consent for those under 18 years old, was obtained from all participants. Liver biopsies of non-BA controls were taken during operations with full

informed consent from parents or patients, and the study was approved by Hong Kong West Cluster-Hong Kong University Cluster Research Ethics Committee/Institutional Review Board (UW 16−052).

2.3. WES and bioinformatics analysis

Genomic DNA was extracted from blood samples for both BA cases and their unaffected parents. We then performed WES on DNA using the xGen Exome Research Panel v1.0 (xGen Lockdown® Probes) (83 BA trios) or TruSeq Exome Enrichment Kit v1.0 (8 BA trios) for exome enrichment, sequenced using the Illumina HiSeq 2000 platform at the Centre for PanorOmic Sciences, University of Hong Kong. Sequence reads were aligned by BWA [15] and processed according to the Genome Analysis Toolkit (GATK) best practice [16] version 3.4 for calling single nucleotide variants (SNVs) and small INDELs. Quality control was performed using PLINK [17] and KGGseq [18] (Supplementary Methods).

2.4. Prioritization of rare, damaging de novo and biallelic mutations in liver-expressed genes

De novo and biallelic variants were first identified using KGGseq. A variant is defined as *de novo* if it is absent in both parents but present in the affected child, while biallelic variants (whether homozygous or compound heterozygous) refer to variants present in both the paternally-inherited and the maternally-inherited copies of the same gene in the affected child. Sanger validation was performed to validate the *de novo* variants. Variants with the same genotype observed in healthy parents as well as the BA probands were excluded (Supplementary Methods). These variants were then annotated in KGGseq with the relevant RefSeq gene features, population allele frequencies in public databases, *in silico* deleteriousness predictions, and known disease associations from the OMIM and ClinVar databases. To prioritize variants of BA association potential, we focused on protein-altering variants that were: (i) rare, (ii) predicted to be functionally damaging and (iii) located in genes expressed in liver or biliary tissues. To define rare variants, population minor allele frequency (MAF; Supplementary Methods) thresholds of < 0.005 for *de novo*, < 0.01 for compound heterozygous variants, and < 0.05 for homozygous variants were used. Functionally damaging variants included all protein-truncating variants and all missense or inframe coding variants that were predicted by SIFT as “deleterious”, by PolyPhen2 as “probably damaging” or that had a CADD score ≥ 20. Candidate gene mRNA and protein expression in liver or bile duct tissue were checked using the human tissue expression database in EMBL-EBI Expression Atlas (www.ebi.ac.uk) and our in-house BA liver organoid expression database [19]. The resulting rare, damaging biallelic variants were visually checked using Integrative Genomics Viewer (IGV). Sanger validation result of selected ciliary *de novo* mutations and IGV plots for those rare, damaging liver expressed biallelic variants in ciliary genes were included as Supplementary Materials, Figs. S1−S3.

2.5. Functional enrichment analysis

Potential disease pathways and molecular mechanisms underlying BA pathogenesis were identified by functional enrichment test of the liver expressed genes with rare, damaging variants against the gene ontology (GO) database, using g:Profiler. Overrepresented functional terms were defined by adjusted p-value < 0.05 [20] after multiple testing correction using the default g:SCS algorithm.

2.6. Ciliary gene set

The list of ciliary genes was derived by combining: (i) SYSCILIA gold standard cilia gene list (303 genes) [21] and (ii) genes with the annotation “cilium” in the GO human database, searched for using AmiGO (791 genes) [22]. The resulting list contained 864 genes involved in ciliary functions with gene products localized within and/or outside the ciliary compartment (Supplementary Materials, Table S1). One-tailed hypergeometric test was performed to evaluate any over-representation of ciliary genes in the set of liver-expressed genes.

2.7. Gene set burden test

We compared the mutation burden of rare, deleterious *de novo* or homozygous variants between 81 (which passed quality check out of 83) BA trios sequenced by xGen Exome Research Panel v1.0 capture kit and 148 ethnicity-matched control trios with non-hepatic congenital condition (8 BA trios enriched by the TruSeq Exome Kit excluded, to minimize any technical variation in sequencing data). Whole genome sequence data of the control trios (mean sequencing depth 39.1x) were processed using identical procedures and software versions to those of the BA variant calling. Quality metrics for sequencing reads and variants in the exonic regions of both cohorts can be found in Supplementary Materials, Table S2. Four gene sets were subjected to burden testing: (a) all protein coding genes exome-wide, (b) all selected ciliary genes in our ciliary gene set (864 genes), (c) liver expressed ciliary genes (586 genes), and (d) non-liver expressed ciliary genes (278 genes). Burden tests were implemented using ProxECAT, a method formulated by the ratio of the counts of functional to non-functional variants, where the counts of non-functional variants are used as a proxy for the confounding effect that may arise from technical variations (e.g. sequencing techniques) in the case-control data [23]. In each gene set, we tested for the difference in the mutation burden of rare, damaging *de novo* and homozygous variants as previously defined, while using the rare, synonymous variants in the corresponding gene set as the non-functional proxy (Supplementary Methods). Unless otherwise specified, all statistical analyses in this study were implemented using the R package.

To assess if the BA phenotype was associated with rare, damaging variants, in each of the four gene sets we carried out logistic regression using Firth’s method on the case-control status. We controlled for any background variation effects by including an individual’s count of rare, synonymous variants in the gene set as covariate.

For multiple testing correction, we used the Benjamini-Hochberg method and obtained the FDR-adjusted p-value, using the *p.adjust* function in R. An FDR-adjusted $P< 0.05$ over the four gene sets was considered to be study-wide significant.

2.8. Immunofluorescence staining of liver sections

For BA patients with ciliary gene mutations of interest (BA634C: *KIF3B* and BA650C: *TTC17*), we examined for the expression of ciliary proteins, acetylated α-Tubulin (1/1000) and pericentrin (PCNT; 1/200), by immunostaining of liver biopsy specimens obtained for diagnostic histopathology from the Kasai procedure or liver transplantation. A total of 11 and 12 bile ducts were examined in liver sections of BA650C and BA634C patients, respectively. Non-tumour liver biopsy specimens from hepatoblastoma (HB) subjects and liver biopsy specimens from choledochal cyst (CC) subjects were used as non-BA controls. Liver biopsies of non-BA controls were taken during operations with full informed consent from parents or patients, and the study was approved by Hong Kong West Cluster-Hong Kong University Cluster Research Ethics Committee/Institutional Review Board (UW 16-052). Liver biopsies of BA patients with no mutation detected in any of the ciliary genes were included as non-mutant BA. Collectively, 83 and 65 bile ducts were examined in non-BA control and non-mutant BA liver sections, respectively. Sections were also immuno-stained for CK19 (1/300) plus PTCH1 (1/50) or GLI1 (1/100) to assay for Sonic Hh signalling in BA and control bile ducts. For details, see Supplementary Methods.

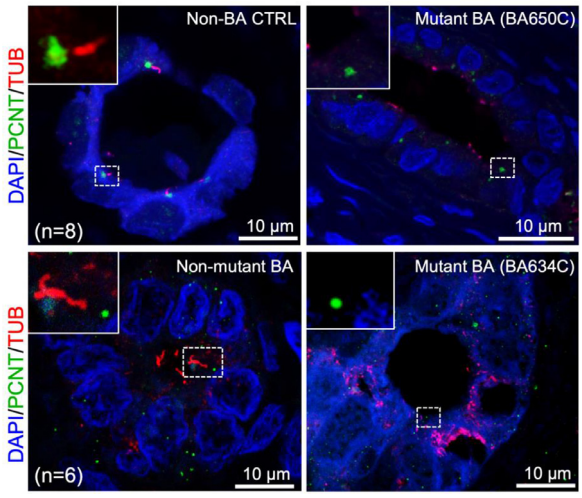

Fig. 1. *Absence of cilia staining in the bile ducts of BA livers of the two patients harboring LOF mutations in the ciliary genes.* Co-immunofluorescence staining for α-Tubulin (TUB; red) and Pericentrin (PCNT; green) was performed on liver sections of Non-BA control (Non-BA CTRL; top left), BA patients with no ciliary gene mutation (Non-mutant BA; bottom left) and BA patients with ciliary gene mutation (Mutant BA; BA650C and BA634C; top and bottom right). α-Tubulin immuno-reactivity was co-localised with PCNT at the luminal surface of the bile ducts of Non-BA CTRL and Non-mutant BA livers. In contrast, only immuno-staining for PCNT were detected but expression of α-Tubulin were absent in BA650C and BA634C patients' bile ducts. Nuclei were stained with DAPI. Representative photos were shown for comparison. Highlighted regions were magnified as shown in inset. Number of patients examined in each group was indicated as "*n*". (For interpretation of the references to color in this figure legend, the reader is referred to the web version of this article).

2.9. Cell culture and transfection

Human foreskin fibroblast cells (BJ, CRL-2522; ATCC) were cultured in DMEM with 10% fetal bovine serum (FBS) and penicillin (100 IU/mL) and streptomycin (100 μg/mL) (Invitrogen). Human intra-hepatic cholangiocytes were derived from liver biopsy via the generation of bile duct organoids following our previously published protocol [19]. Human cholagniocytes were cultured as a monolayer on cover slip coated with Matrigel (356231; Corning Biocoat) in organoid medium until ready for short interfering RNAs (siRNA) transfection. The siRNAs specifically target to *PCNT, KIF3B, TTC17* and control-scrambled siRNA were purchased from Santa Cruz Biotechnology. The fibroblast cells and human cholangiocytes were transfected with siRNAs via Lipofectamine® RNAiMAX reagent (Life technologies) according to the manufacturer's instructions. Fibroblast cells were grown to 80% confluence on the day of transfection and starved of serum for 48 h. Human cholangiocytes were grown to 80% confluence on the day of transfection in organoid medium.

2.10. Scanning electron microscopy

For cilia imaging by scanning electron microscopy (SEM) of human cholangiocytes, at 48 h post siRNA transfection, the culture medium was removed and the cholangiocytes were fixed in 4% PFA/PBS (paraformaldehyde in phosphate buffered saline) for 16 h, dehydrated in a series of graded ethanol until 100% (EM grade) and processed for SEM analysis by Electron Microscopy Unit (EMU) of the Queen Mary Hospital, Hong Kong following standard protocols. Samples were examined on Hitachi S-4800FEG (Tokyo, Japan) and LEO 1530 FEG (Georgia Tech, Georgia Institute of Technology, Atlanta, USA) scanning electron microscopes. At least 50 cells in each siRNA transfected culture were examined for the presence of cilia and the percentage of ciliated cells in each transfected cultures were quantified. Each siRNA transfection were performed in duplicate.

2.11. Real-time PCR

RNA was isolated from BJ cells with RNeasy Mini Kit (Qiagen) and reverse-transcribed with PrimeScript™RT reagent Kit with gDNA Eraser (Takara). Samples were assayed with iTaq™ Universal SYBR Green Supermix (Bio-Rad). Real-time PCR was performed with ViiA 7 (Applied Biosystems). Relative expression levels of *PCNT, KIF3B* and *TTC17* in transfected cells were determined using glyceraldehyde 3-phosphate dehydrogenase (*GAPDH*) as internal reference and $2^{-\Delta\Delta Ct}$ method. The relative fold change of expression between scrambled and *PCNT, KIF3B* and *TTC17* siRNA transfected cells were calculated taking the relative expression level of *PCNT, KIF3B* and *TTC17* in scrambled siRNA transfected cells arbitrarily as one, and expressed as mean ± standard deviation (SD).

2.12. Immunofluorescence staining of cells

The cells were fixed with 4% PFA and incubated with anti-acetylated-α-tubulin (1/1000) and anti-PCNT (1/200) antibodies. Alexa Fluor® 488-conjugated goat anti-rabbit IgG and Alexa Fluor® 594 goat anti-mouse IgG secondary antibodies (1/300, Invitrogen) were used. Cells were then counterstained with DAPI. Confocal images were captured with the Carl Zeiss LSM 880 microscope. Image processing was performed with the ZEN 2.3 software. Images were analyzed with Image J.

2.13. CRISPR/Cas9 gene knockout in zebrafish model

We used wildtype zebrafish and transgenic zebrafish (Danio rerio) lines (um14Tg[Tg(tp1-MmHbb:EGFP)um14] (ZL1950; Zebrafish International Resource Center (ZIRC), 5274 University of Oregon, Eugene, OR 97403−5274, USA)) as animal models to investigate the *in vivo* association between candidate ciliary genes and the BA phenotype, by CRISPR/Cas9 gene knockout. The um14Tg[Tg(tp1-MmHbb:EGFP)um14] transgenic fish expressed strong green fluorescent protein signal in bile ducts and were used to investigate the biliary development in zebrafish [24–27]. Bile flow was assessed in 51−57 independently injected embryos per wildtype or gene-knockout test group, by measuring the ability to process N-([6-(2,4-dinitro-phenyl)amino]hexanoyl)-1-palmitoyl-2-BODIPY-FL-pentanoyl-sn-glycerol-3-phosphoethanolamine (PED6) [28], a fluorescent lipid reporter for examination of biliary function. We cultured gRNA-injected and un-injected embryos until 5 days post-fertilization, after which they were released to swim in a 5 μM solution of PED6 for 2 h. During this period, images using an Olympus SZX7 fluorescent microscope with fixed fluorescence intensity were taken at the same magnification with identical brightness and contrast settings at 30 min intervals. We analysed the microscopic images using ImageJ [29]. The total green fluorescence in the gall bladder was calculated as integrated density (area × mean fluorescence intensity). Comparison of PED6 uptake between each mutant embryo group and wild type was performed using *t*-test. $P < 0.05$ was considered to be statistically significant.

2.14. Measurements of nNO, ciliary beat frequency, beat pattern and ultrastructure

Ten BA patients identified to have rare, damaging ciliary mutations could be recalled and agreed to further clinical evaluation. We performed tidal breathing nNO (TB-nNO) test using NIOX® (Nitric Oxide Monitoring System) MINO hand-held electrochemical device sampling at flow rates of 2 ml/s (MINO2) or 5 ml/s (MINO5) on these patients. Nasal NO concentrations were measured with non-velum closure techniques in parts per billion (ppb) and were compared against the device-specific ranges previously published for healthy and primary ciliary dyskinesia (PCD) subjects [30]. Ciliated epithelial samples were obtained by brushing the inferior nasal turbinate. Ciliary beat frequency (CBF) and beat pattern were analyzed using high speed video microscopy (HSVM) while ciliary ultrastructure were assessed using TEM as described

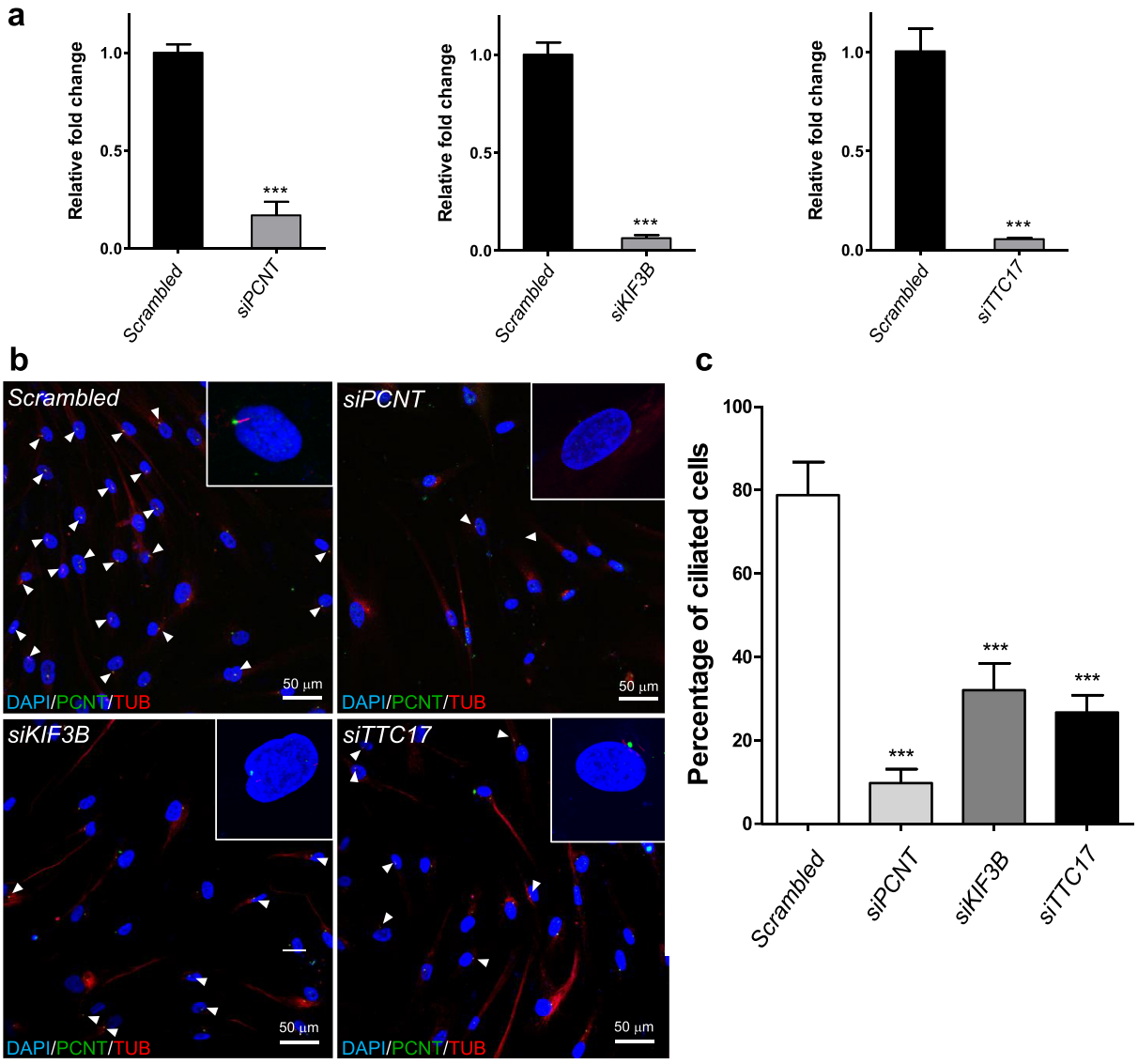

Fig. 2. Knockdown of *PCNT, KIF3B* and *TTC17* resulted in reduced number of cilia in cells. (a) Examination of the knockdown efficiency by siRNAs in human fibroblasts by real-time quantitative PCR assay using *GAPDH* as internal controls. Three independent experiments were performed and data represented as means ± standard deviation (SD). *** $p < 0.0001$, two-sided *t*-test. Cells transfected with non-specific *scrambled siRNA* were employed as negative controls and relative expression levels of *PCNT, KIF3B* and *TTC17* to *GAPDH* in *scrambled siRNA* transfected cells were arbitrarily regarded as 1. (b) Effect of *PCNT, KIF3B* and *TTC17* knockdown on cilia. Cells were transfected with *siRNAs* and serum-starved for 48 h, then immuno-stained for acetylated-α-tubulin (TUB; red) and pericentrin (PCNT, green). Nuclei were stained with DAPI (blue). Representative images of each of the *siRNA* transfection were shown. Ciliated cells (arrowheads) were abundant in *scrambled siRNA* transfected cells, whereas ciliated cells were scarce in *siPCNT, siKIF3B* and *siTTC17* transfected cells. Ciliated cell and non-ciliated cells were magnified as shown as inset. (c) Percentage of ciliated cells in *scrambled siRNA, siPCNT, siKIF3B* and *siTTC17* transfected cells was determined by counting ciliated cells and total number of cells. Two independent transfection experiments were performed for each siRNA, and over 100 cells were counted in each experiment. Data was shown as means±SD. *** $p < 0.0001$, one-way ANOVA, two-sided test. All scale bars = 50 μm. (For interpretation of the references to color in this figure legend, the reader is referred to the web version of this article).

previously [31] (See Supplementary Methods). The CBF, beat pattern, and ultrastructure of the ciliated epithelium and ciliary axonemes of the BA patients were compared against the normal age-related healthy reference ranges established on Chinese children and adults [31].

2.15. Role of funding source

Funders had no role in study design, data collection, data analyses, interpretation, or writing of the manuscript.

3. Results

WES was performed on 91 Southeast Asian nonsyndromic BA trios, each with one affected patient plus their two unaffected parents. A total of 89 BA trios passed quality controls and were subject to genetic analysis. The mean and median sequencing depths were 31.9x and 28x, respectively.

3.1. Most BA cases carry rare, damaging de novo or biallelic (RDL) variants in liver expressed genes

To identify potentially pathogenic variants, we filtered **R**are, **D**amaging protein-altering variants present in the BA proband but not in their unaffected parents and in genes expressed in **L**iver/biliary tissues (hereafter known as RDL variants). Among 92% of the BA subjects (n = 82), we identified 45 *de novo* RDL variants, of which 8 were predicted to cause loss-of-function (6 stopgain and 2 frameshift), and 233 biallelic (112 homozygous and 121 compound heterozygous) RDL variants,

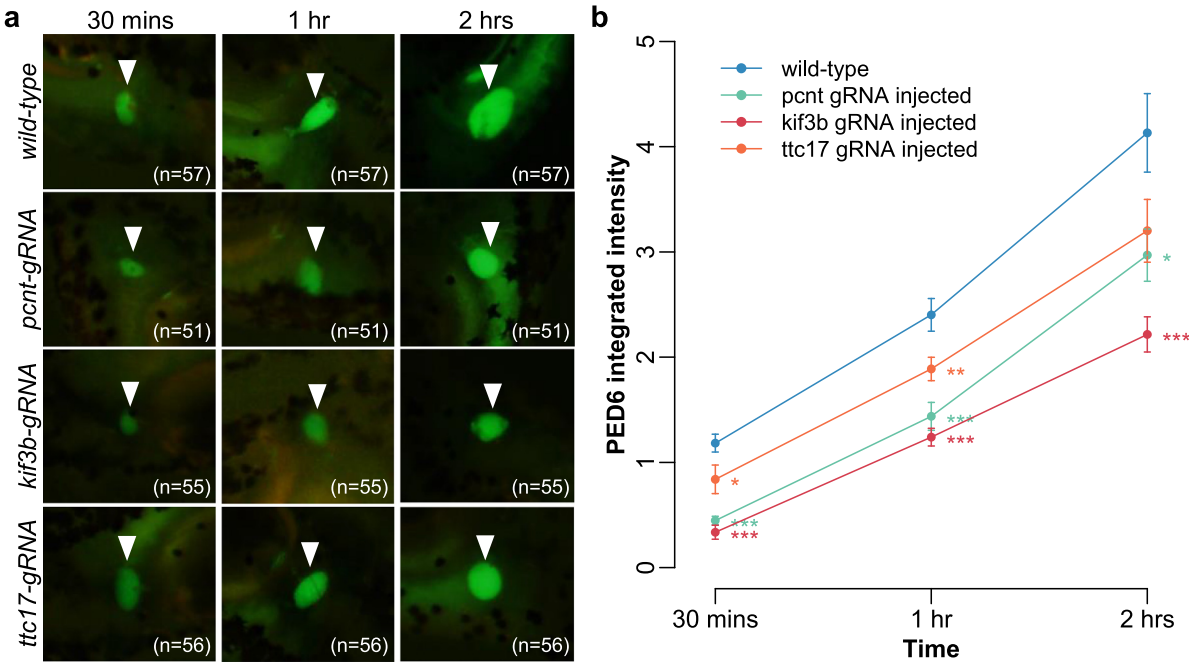

Fig. 3. Knockout of *pcnt, kif3b* and *ttc17* resulted in defective bile flow in mutant zebrafish. (a) Representative epifluorescence images and (b) line plot of *pcnt* (n = 51), *kif3b* (n = 55) and *ttc17* (n = 56) mutant embryo groups at 5 days post-fertilization showing significantly lower accumulated PED6 integrated density in gallbladder (arrowhead) after incubation for 30 min (left), 1 h (middle) and 2 h (right) compared to wild type (n = 57). Data expressed as mean ± standard error of the mean (SEM). Results of pairwise t-test: ***, $P < 0.001$; **, $P < 0.01$, *, $P < 0.05$.

distributed in 239 genes. Of these 239 genes, none had been linked to any form of BA in previous studies nor case reports [14]. Only *PKHD1* that was found to have a biallelic variant in one of our BA patient was screened in a previous study of perinatal BA patients, but no pathogenic mutation was found [32]. Three genes had multiple RDL variants observed in > 2 BA patients but all of which are predicted as being tolerant to missense mutations according to the constraint score (missense z-score: *TTN*, -1.10; *PLEC*, -2.57; *USH2A*, -2.47).

3.2. Ciliary genes are enriched for RDL variants in BA patients

To gain insights into the major biological or molecular functions associated with these 239 RDL genes, we performed functional enrichment analysis using g:Profiler. We detected seven highly related GO biological processes that were significantly enriched with RDL variants (adjusted $P < 0.05$; Table 1), namely cytoskeleton organization, cilium organization, microtubule cytoskeleton organization, microtubule-based process, cilium assembly, spindle organization, and organelle assembly, covering ~20% (= 49/239) of the RDL genes and half of (n = 26) which are ciliary genes. Similar enrichment of GO molecular function terms were observed. In fact, microtubule is an integral part of both cytoskeleton and cilia. It is a core component of the cilium axenome and is essential in cilia assembly and in the regulation of ciliogenesis. Specially, among the eight genes with protein truncating *de novo* mutations that are considered as most pathogenic, around 37.5% (n = 3; *KIF3B, PCNT,* and *SPEF2*) were ciliary genes (Supplementary Materials, Table S3). Strikingly, 31.5% (28/89) of the BA subjects carried at least one RDL variant in ciliary genes. The genetic profiles of these RDL ciliary variants in BA patients were given in Supplementary Materials, Table S4. To further delineate if the enrichment of cilia-related GO terms could be biased simply due to the selection of genes expressed in liver, we performed hypergeometric test but did not find overrepresentation of ciliary genes in liver-expressed gene set (P = 1.0). This implies that the GO enrichment is specific to genes identified to contain rare, *de novo* or biallelic deleterious variants in BA patients. These findings corroborated with previous report of association of *PKD1L1,* also a ciliary gene, with syndromic BA-BASM, leading us to hypothesize that the cilium is the key organelle affected by the genetic mutations observed in nonsyndromic BA subjects [13].

3.3. Excess of rare deleterious variants in ciliary genes compared to controls

To further confirm the excess of ciliary mutations in nonsyndromic BA patients, we performed gene set burden tests for rare, *de novo* and homozygous variants relative to 148 population control trios by ProxECAT and logistic regression while adjusted for counts of rare synonymous variants. Considering all protein coding genes, no enrichment of these rare deleterious mutations was found in patients (odds ratio (OR) [95% CI]=1.12 [0.93−1.35], false discovery rate (FDR) adjusted P [P-adjusted]= 0.241; ProxECAT: P-adjusted= 0.484), demonstrating the comparability of the case-control data (Table 2). In contrast, when we considered only the liver expressed ciliary genes, both tests consistently detected case-control differences and the presence of an RDL ciliary variant increased risk of BA by 2.6-fold (OR [95% CI]= 2.58 [1.15−6.07], P-adjusted = 0.034; ProxECAT: P-adjusted = 0.048). Results for non-liver expressed ciliary genes were mixed and the inconclusive result is probably due to the sparse variant counts in that gene set (around 5 synonymous/nonsynonymous variants in the whole control cohort, Table 2) and/or the difference in statistical power between the two methods. Irrespective of the gene expression in liver tissues, excess burden was observed in patients for all ciliary genes by both methods (OR [95% CI]= 3.24 [1.63−6.67], P-adjusted = 0.030; ProxECAT: P-adjusted = 0.048). Further stratification of the patients by ancestries (Chinese versus Vietnamese) and by sex detected no difference between groups, implicating the robustness of the enrichment (Supplementary Materials, Table S5).

3.4. High level of locus heterogeneity in nonsyndromic BA involving diverse ciliary functions

For our nonsyndromic BA patients, instead of having excess mutations in a single or a few major ciliary genes, there is high level of

Table 1
Results of gene set enrichment analysis on 239 genes with RDL variants. List of overrepresented GO biological process and molecular function with adjusted *p*-value < 0.05.

Term description	GO term ID	Gene count	*P*
GO biological process			
Cytoskeleton organization [a,b,c]	GO:0007010	39	1.09×10^{-3}
Cilium organization [a,b,c]	GO:0044782	18	3.22×10^{-3}
Microtubule cytoskeleton organization [a,b]	GO:0000226	22	4.23×10^{-3}
Microtubule-based process [a,b]	GO:0007017	26	5.84×10^{-3}
Cilium assembly [a,b]	GO:0060271	17	7.24×10^{-3}
Spindle organization [a,b]	GO:0007051	11	2.08×10^{-2}
Organelle assembly [a,b,c]	GO:0060271	26	3.38×10^{-2}
GO molecular Function			
Cytoskeletal protein binding [a]	GO:0008092	34	4.09×10^{-5}
Cell adhesion molecule binding	GO:0050839	20	2.82×10^{-3}
Protein-containing complex binding [a]	GO:0044877	31	1.68×10^{-2}
Ankyrin binding	GO:0030506	4	4.50×10^{-2}

[a] denotes the enriched GO term containing *KIF3B*.
[b] denotes the enriched GO term containing *PCNT*.
[c] denotes the enriched GO term containing *TTC17*.

locus heterogeneity in which multiple occurrence of these RDL variants per ciliary gene was sparse (only *DNAH8, PKD1* and *USH2A* with RDL variants in > 1 BA cases; Table 3 and Supplementary Materials, Table S4). A broad spectrum of ciliary genes with diverse localizations and ciliary functions were involved (Table 3). For example, PCNT located at the basal body that forms the pericentriolar material, a nucleation site for microtubules, is involved in cilia assembly. The GLI1 transcription factor on the axoneme mediates the Hedgehog (Hh) pathway while KIF3B is an essential anterograde intraflagellar transport (IFT) motor driver for cilia assembly and maintenance. On the other hand, TTC17 localizes outside the ciliary compartment and is involved in actin organization and pre-ciliogenesis. To evaluate the potential impact of the ciliary mutations on cilia structure and BA phenotypes, we selected three ciliary genes affected by *de novo* mutations in our BA probands—*KIF3B, PCNT* and *TTC17*—as the representatives of key ciliary localizations and functions in cilia assembly for functional characterization.

3.5. Abnormal cilia in the bile ducts of BA patients

We first examined if the ciliary mutations correlated with cilia formation in the bile duct of the corresponding BA patients. We examined the cilia marker co-immunofluorescence staining of the BA livers for patients carrying *de novo* stopgain and missense RDL variants in *KIF3B* (BA634C) and *TTC17* (BA650C), respectively compared to the liver biopsies of non-BA controls (total n=8; including biopsies of non-tumor liver of hepatoblastoma (HB; $n = 4$), liver of choledochal cysts (CC; $n = 4$)), and non-mutant BA subjects without ciliary mutation ($n = 6$) (Fig. 1). In contrast to an average of 3.6 ([S.E.M.] ± 0.1) and 3.2 ([S.E.M.] ± 0.1) cilia detected per bile duct in non-BA control and non-mutant BA livers, respectively, cilium axoneme were absent in all bile ducts ($n = 11$ and 12) of the both mutant BA subjects. BA634C has two *de novo* ultra-rare stopgain RDL variants not present in any public databases, one in *KIF3B* and another in *SPEF2*. *SPEF2* is known to function in motile cilia, especially for sperm development and tracheal cilia beating, since depletion in *SPEF2* causes male infertility and primary ciliary dyskinesia (PCD) in mice [33]. Therefore the absence of primary cilia in cholangiocytes was more likely to be attributed to the *KIF3B* mutation. The liver tissue sample of the BA subject with *PCNT* mutation was not available, but a previous study reported that PCNT depletion results in loss of primary cilia in human epithelial cells [34]. Given the importance of primary cilia in Hh signaling pathway in cholangiocytes, we further examined the expression of sonic Hh markers, PTCH1 and GLI1, in the bile ducts of these two BA subjects and compared the expression to those of non-BA control (HB, $n = 3$; CC, $n = 3$) and non-mutant BA ($n = 9$) subjects. Dysregulation of PTCH1 and GLI1 were observed in both mutant BA subjects (Supplementary Materials, Fig. S4), suggesting correlation between abnormal cilia and aberrant Hh regulation in mutant BA patients.

3.6. Gene knockdown resulted in reduction in number of cilia in human fibroblast and cholangiocyte cells

To directly assess the impact of loss of function of these ciliary genes, we further knocked down *KIF3B, PCNT* and *TTC17* by siRNA transfection in human control cholangiocyte and fibroblast cells. A significant reduction in the number of ciliated human fibroblast cells was observed compared to controls transfected with non-specific scrambled siRNA (Fig. 2). Effect of siRNA knockdown on cilia of human cholangiocytes were also investigated by SEM analysis. Under SEM examination, primary cilia appeared as a long and thick protrusion from the cholangiocyte cell surface as compared to the surrounding short and thin microvilli (Supplementary Materials, Fig. S5). Primary cilia could be identified in 40-50% of cells in scrambled siRNA transfected cultures (Supplementary Materials, Fig. S5a). In contrast, cilia were either undetected or detected at lower percentages in *KIF3B, PCNT* and *TTC17* siRNA transfected cultures (0-2% in *KIF3B* siRNA transfected cultures; 0% in *PCNT* siRNA transfected cultures; 10−12% in *TTC17* siRNA transfected cultures) (Supplementary Materials, Fig. S5b,c and data not shown). This reduction in the number of ciliated human cholangiocyte cells compared to controls transfected with non-specific *scrambled siRNA* (Supplementary Materials, Fig. S5) further confirmed the effect of abnormal cilia formation caused by the depletion of the selected ciliary genes.

3.7. Ciliary gene knockout leads to impaired biliary function in zebrafish

We next assessed if ciliary gene depletion could cause BA phenotype *in vivo* using zebrafish model. Knockout of *pcnt, kif3b* and *ttc17* was performed by CRISPR/Cas9-mediated genome editing. Introduction of INDEL in *pcnt, kif3b* and *ttc17* genes was confirmed by T7E1 assay and reduced expression of *pcnt, kif3b* and *ttc17* in injected embryo was demonstrated by semi-quantitative RT-PCR (Supplementary Materials, Fig. S6). The biliary development of un-injected (Cas9 protein alone) and *pcnt*-, *kif3b*- and *ttc17*- gRNA injected 5-dpf um14Tg[Tg(tp1-MmHbb:EGFP)um14] larvae were studied by examining the bile duct green fluorescence signal intensity under fluorescence microscope. Zebrafish larvae with the knockout of *pcnt, kif3b* and *ttc17* showed comparable biliary green fluorescence signal as control larvae, which suggested that knockout of these genes did not cause gross abnormal bile duct development in zebrafish (Supplementary Materials, Fig. S7). To further examine the impact of the knockout of *pcnt, kif3b* and *ttc17* on bile flow from liver to the gall bladder in zebrafish, we performed PED6 bile flow assay in *pcnt, kif3b* and *ttc17* knockout non-transgenic fish. Knockout of all three genes resulted in defective bile flow in fish embryos, as measured by significantly lower integrated density of PED6 in the gall bladder in the embryo mutant groups compared to the control group (Fig. 3). This demonstrated that BA-like phenotype of impaired bile blow in zebrafish model can be ascribed to disrupted function of *PCNT, KIF3B* and *TTC17*.

3.8. Impaired respiratory ciliary function in majority of patients with RDL variants

Clinically, disorders of cilia dysfunction often present with complex multisystem involvement. Although nonmotile ciliopathies are clinically distinct from motile ones (e.g. PCD), they sometimes display common clinical features, including hepatobiliary and kidney diseases, due

Table 2
Mutation burden of rare, damaging *de novo* and homozygous variants in 4 gene sets: (a) all protein coding genes, (b) all ciliary genes (n = 864), (c) liver expressed ciliary genes (n = 586), and (d) non-liver expressed ciliary genes (n = 278), in 81 BA trios compared to 148 ethnicity-matched control trios.

	All genes		Ciliary genes					
			Overall		Liver expressed		Non-liver expressed	
	BA	Control	BA	Control	BA	Control	BA	Control
Per-person rare mutation count (mean)								
Synonymous (*S*)	2.19	2.24	0.14	0.15	0.08	0.11	0.06	0.03
Damaging non-synonymous (*dNS*)	2.25	2.01	0.29	0.10	0.18	0.07	0.11	0.03
dNS/S	1.03	0.90	2.09	0.68	2.33	0.59	1.80	1.00
ProxECAT								
P [a]	0.364		**0.021**		**0.024**		0.484	
FDR-adjusted *P* [b]	0.484		**0.048**		**0.048**		0.484	
Logistic regression								
Odds ratio (95% CI) [c]	1.12 (0.93-1.35)		**3.24 (1.63-6.67)**		**2.58 (1.15-6.07)**		**3.36 (1.16-10.70)**	
P [a]	0.241		**0.007**		**0.021**		**0.026**	
FDR-adjusted *P* [b]	0.241		**0.030**		**0.034**		**0.034**	

[a] *P*-value of gene set burden test (< 0.05 in bold) before multiple comparison adjustment.
[b] FDR-adjusted *p*-value (< 0.05 in bold) of the gene set burden test derived by Benjamini-Hochberg method.
[c] Odds ratio from logistic regression on the case-control status (in bold: both *P* and FDR-adjusted *P* < 0.05). CI, confidence interval.

to the common involvement of ciliary processes and underlying signaling defects between the motile and primary cilia [35]. Prior to this WES, we came across a syndromic BA patient with dextrocardia and situs invertus. The patient was suspected to have PCD and displayed high proportion of disarranged respiratory cilia upon respiratory ciliary test. Thus, we attempted to use a simple non-invasive nNO test, a well-established first line screening test for PCD, on those BA patients with RDL variants to indirectly assess ciliary dysfunction clinically [36]. PCD patients with abnormal ciliary structure and/or function have exceptionally low nNO levels. NO biosynthesis depends on nitric oxide synthases (NOS) and NOS activity relies on normal ciliary function [37,38]. Production and release of NO may depend on the activation of cilia in response to fluid flow-generated shear stress and thus measures of NO concentration may indirectly reflect ciliary function and signaling [39]. Surprisingly, as shown in Table 4, eight out of the 10 BA patients with ciliary mutations have abnormally low nNO levels. Four patients have nNO levels in the range suggestive for PCD while the other four patients have low nNO levels outside the normal range of healthy subjects. While motile respiratory cilia ultrastructure abnormalities detected by TEM were within the normal range (Supplementary Materials, Fig. S8) and the average ciliary beat frequencies (CBF) and beat pattern detected using HSVM also appeared normal for all 10 BA patients, detailed side-view visual examinations revealed that three patients have their CBF recorded at the lower end (<=7.5 Hz) in a proportion of edges (1−3 in 10). Representative high speed videos of a BA patient with abnormal CBF and a healthy subject were included in Supplementary Materials, video S1 and S2. Altogether, the low nNO levels and abnormal CBF for a subset of respiratory motile cilia suggested subtle impaired ciliary function in BA patients with ciliary mutations and highlighted the plausible multiorgan involvement in this patient subgroup.

4. Discussion

BA clinically presents with obstruction, inflammation and fibrosis in the biliary tree and is widely considered as multifactorial in origin, involving poorly defined environmental and genetic factors. In this largest WES study on nonsyndromic BA trios to date, we found an excess burden of rare, deleterious mutations carried by BA patients, in a wide spectrum of liver expressed ciliary genes that play different roles in ciliary function and ciliogenesis. Cilia were found absent in the liver of our BA patients with *KIF3B* or *TTC17* mutations and the corresponding zebrafish mutants (including *PCNT*) exhibited impaired biliary function. We further demonstrated reduction of cilia formation caused by the depletion of these genes independent of the genetic background of the patients, which were consistent with other experimental studies [34,40−42]. Clinical evaluation by nNO test revealed abnormally low level of nNO in a majority (80%) of BA patients with ciliary mutations, implicating intrinsic ciliary defects and highlighting a subset of patients with potential pleiotropic phenotypes. Based on these findings, we suggest that genetic factors play a major role in a substantial proportion of nonsyndromic BA cases. Our findings also implicate defective ciliary structure and function as one of the underlying mechanisms of BA pathogenesis.

We hypothesize that ciliary gene mutations can lead to the development of BA phenotypes through two interconnected biological mechanisms. First, it was suggested that defective cholangiocyte cilia structure and function can in itself cause dysregulation of the Hh pathway, which promotes dysfunctional tissue repair and leads to hepatic inflammation and fibrogenesis [43]. The primary cilium is indispensable in the Hh signaling pathway both physiologically and biologically, interacting with various components at different points of the signaling cascade to regulate liver regeneration and repair. The Hh ligand receptors and transcription factors depend on primary cilia for activation, mediation and suppression, and the core signaling components are localized to cilia, thus requiring IFT for their trafficking to the functional sites for regulatory activities [44]. However, there have been growing evidence that non-canonical pathway under the absence of cilia was also involved in liver pathophysiology progressed from chronic liver injury [44,45] and tumorigenesis [46]. Secondly, it is likely that defective cilia would compromise the protective function of immature neonatal cholangiocytes against bile acid insults, leading to chronic liver injury, which can also trigger Hh signalling. In different tissue types, aberrant or absent cilia, or mutations in IFT proteins were shown to cause Hh loss- or gain-of-function phenotypes [46,47]. Indeed, shorter, misoriented, or less abundant cholangiocyte cilia were commonly observed in several studies of both syndromic and nonsyndromic BA patients [48−50], meanwhile Hh activity was shown to be associated with jaundice-free survival of BA patients in another study [51]. Our current study is the first to suggest genetic defects might underlie these observations in nonsyndromic patients. We showed convincing evidence that at least some of the nonsyndromic patients with rare damaging mutations in ciliary genes have no primary cilia in their bile ducts and concurrently with deregulated Hh signaling. Elucidating the molecular mechanisms by which the defective primary cilium dysregulate Hh signaling may provide a better understanding of the disease pathogenesis and offer potential targets for alternative therapies.

Table 3
List of 26 ciliary genes with RDL variants in the BA probands categorized by ciliary localization and functions.

Gene	Description	Localization / functional category	Ciliopathy association [a]	Inheritance [b] [> 1 case]
KIF3B	kinesin family member 3B	IFT-kinesin		*De novo*
DNAH8	dynein axonemal heavy chain 8	Outer dynein arm	Spermatogenesis defects	Homo [2]
BBS9	Bardet-Biedl syndrome 9	BBSome-IFT-associated, basal body	Bardet-Biedl syndrome 9	Homo
GLI1	GLI family zinc finger 1	Axoneme (tip), transcription factor		CompHet
MYO15A	myosin XVA	Axoneme (tip)		CompHet
TEKT4	tektin 4	Axoneme	Asthenozoospermia (M); subfertility (M)	Homo
PKD1	polycystin 1, transient receptor potential channel interacting	Axoneme, membrane - signaling	ADPKD	CompHet [2]
PKHD1	PKHD1 ciliary IPT domain containing fibrocystin/polyductin	Axoneme, basal body - signaling	ARPKD	CompHet
TTLL3	tubulin tyrosine ligase like 3	Axoneme modification		CompHet
PCNT	pericentrin	Centrosome	Microcephalic osteodysplastic primordial dwarfism, type II	*De novo*
HAUS1	HAUS augmin like complex subunit 1	Centrosome		Homo
CLASP1	cytoplasmic linker associated protein 1	Centrosome; microtubule plus-end		Homo
CEP131	centrosomal protein 131	Centriolar Satellite		*De novo*
PCM1	pericentriolar material 1	Centriolar Satellite		CompHet
SPAG17	sperm associated antigen 17	Central Pair		CompHet
SPEF2	sperm flagellar 2	Central Pair	Spermatogenesis defects (M); PCD (M)	*De novo*
USH2A	usherin	Basal body	Usher syndrome; retinitis pigmentosa	CompHet [3]
DCTN1	dynactin subunit 1	Subdistal appendage, basal foot	ALS; Perry syndrome; neuropathy, distal hereditary motor, type VIIB	CompHet
TTC17	tetratricopeptide repeat domain 17	Actin filament polymerization		*De novo*
DHRS3	dehydrogenase/reductase 3	Membrane		Homo
PROM1	prominin 1	Membrane, endoplasmic reticulum		Homo
NOTCH1	notch receptor 1	Signalling		CompHet
PKHD1L1	PKHD1 like 1	Signalling		CompHet
SYNE2	spectrin repeat containing nuclear envelope protein 2	Trafficking, actin remodeling	Emery-dreifuss muscular dystrophy 5	Homo, CompHet
EXOC6	exocyst complex component 6	Exocytosis - vesicle docking		Homo
LAMA5	laminin subunit alpha 5	Extracellular - integrin binding		CompHet

[a] Abbreviation: (M), phenotypes specific to mice; ADPKD, Autosomal dominant polycystic kidney disease; ALS, Amyotrophic lateral sclerosis; ARPKD, autosomal recessive polycystic kidney disease; BBSome, Bardet-Biedl syndrome complex; IFT, intraflagellar transport; PCD, primary cilia dyskinesia.
[b] Mutation type: Homo, homozygous; CompHet, compound heterozygous. Number in brackets indicates case count (> 1) of RDL variants.

One of the interesting findings is the low nNO levels in 80% of BA patients with ciliary mutations. Although primary cilia (cholangiocyte cilia) are structurally and functionally distinct from motile cilia (respiratory cilia), the similarity in cilium–centrosome complex and the shared signaling pathways (e.g. Hh signaling) across tissues with ciliated cells may account for the involvement of multiple organ systems in ciliopathies generally. Genetic predisposition to dysregulation of liver-expressed ciliary genes may thereby exert a functional impact beyond the hepatobiliary system. Such predisposition may not be necessarily sufficient for clinical manifestation as a ciliary defect in nonsyndromic BA patients, rather milder or subclinical phenotypes may reside and other modifiers (genetic or environmental factors) can play a pathogenic role in triggering ciliary dysfunction. This finding suggested a further follow up and thorough clinical assessment of this patient subgroup for any pleiotropic clinical features to establish genotype-phenotype correlation and to improve clinical management and disease outcome.

Familial aggregation of BA is rare with low recurrence in siblings, even among monozygotic twins [52]. Mendelian form of inheritance of rare causal variants with high penetrance is therefore unlikely to account for the majority of BA etiology. Unlike syndromic BA with laterality defects that can be caused by high penetrant ciliary mutations similar to other ciliopathies, we hypothesize that RDL ciliary mutations confer a strong genetic predisposition to risk of nonsyndromic BA and provide a sensitized genetic background such that other genetic and/or environmental factors may act as modifiers of penetrance or triggers for the disease manifestation. The synergistic effect of genetic modifier(s) has been demonstrated in classical zebrafish model of BA in which knockdown of both Egfr and Arf6 of the same signaling pathway resulted in a more severe biliary defect compared to minimal or no defects in intrahepatic biliary structure when knockdown each gene alone [12]. Inherited common genetic variations in BA susceptibility genes, e.g. *ADD3* and *GPC1*, may further contribute to the genetic susceptibility and disease expressivity through perturbation of interconnected biological pathways including Hh signaling [8,10,53]. Compared to the multiple occurrence of rare damaging biallelic variants in a single gene, *PKD1L1*, in syndromic patients with BASM, the scarce multiple occurrences observed for individual variants or genes in nonsyndromic BA patients has important implications on future genetic analyses of this patient subgroup. Unlike the syndromic form, the nonsyndromic BA is unlikely to have a single genetic etiology. Instead of focusing on mutational burden on single gene-level, the genetic heterogeneity of nonsyndromic BA calls for a gene set-based enrichment analysis aggregating genetic effects across multiple genes in pathways or biological meaningful gene sets and possibly a more lenient damaging criteria to detect the strong predisposing effect. Examining mainly the top 0.1% damaging novel variants transmitted in a Mendelian fashion might partially account for the lack of genetic association for a recently published WES study on nonsyndromic BA [54].

The genetic contributions to cholangiocyte ciliary malformation and ciliary protein dysfunction appear to be heterogeneous, demonstrated by the diverse spectrum of liver expressed ciliary genes identified to carry RDL variants in BA cases in this study. We found almost a third of BA subjects with rare, damaging, liver expressed ciliary gene variants, whilst a previous descriptive histopathological study observed cilia abnormalities in 86% of BA subjects [49]. The considerable gap could be attributed to the ciliary gene list we applied is relatively conserved, including only genes from SYSCILIA gold standard and GO databases for a list of confident ciliary genes, but not the candidate genes in other databases where stronger evidence of their ciliary nature are yet to be established. It could also be that the genetic variations in the non-coding regions contribute to cilia abnormality. Further genetic studies using whole genome sequencing along with

Table 4
Analysis of ciliary beat frequency (CBF) and nasal nitric oxide (nNO) levels for 10 BA patients with rare deleterious ciliary mutations.

	Ciliary mutation				HSVM[c]		nNO test	
Subject ID	Inheritance mode[a]	Gene	Amino acid change[b]	Testing Age(years)	Mean CBF (Hz)	Number of edges (out of 10) with visual CBF <=7.5	Hand-held analyzer	nNO concentrations (ppb)[d]
BA171C	CompHet	*MYO15A*	p.V2872M/p.I3421M	18	11.7	0	MINO5	341
BA230C	CompHet	*NOTCH1*	p.G1195R/p.T1035S	13	10.7	0	MINO5	**185**
	CompHet	*PKD1*	p.R3046C/p.S1679R					
BA307C	Homo	*PROM1*	p.S281R	11	9.5	3	MINO2	**152**
BA596C	CompHet	*USH2A*	p.R1870W/p.T3014N	8	11.4	0	MINO2	853
	Homo	*DNAH8*	p.E972V					
BA611C	CompHet	*USH2A*	p.C729*+ p.S333P /p.A3438T	7	9.4	0	MINO2	**168**
BA613C	CompHet	*PKD1*	p.S699L/p.R2075C	7	11.5	1	MINO2	***25***
BA634C	*De novo*	*KIF3B*	p.R153*	7	9.2	2	MINO2	***27***
	De novo	*SPEF2*	p.Y473*					
BA636C	Homo	*CLASP1*	p.S617P	6	9.5	0	MINO2	***29***
BA642C	CompHet	*PCM1*	p.T1174A/p.T1513S	5	11.3	0	MINO2	**102**
BA645C	Homo	*DNAH8*	p.E972V	5	12.8	0	MINO2	***16***

[a] CompHet: Compound heterozygous; Homo: Homozygous
[b] Amino acid changes for compound heterozygous variant are ordered by paternal/maternal inheritance
[c] HSVM: high speed video-microscopy; The ranges (5th - 95th percentiles) of CBF are (i) 6.3 − 13.5 and (ii) 5.5 − 11.9 for healthy subjects with age (i) under 18 and (ii) above 18, respectively as reported in Lee et al.[31].
[d] Ppb:parts per billion; BA patients with nNO levels lower than the 1 standard error (SEM) of healthy subjects are bolded and those within the range of 1 SEM of primary ciliary dyskinesia (PCD) patients are italicized. The ranges (±1 SEM) of nNO levels are (i) 4 − 72 and (ii) 317 − 363 for (i) PCD patients and (ii) healthy subjects, respectively using hand-held analyzer MINO5 and (iii) 51 − 97 and (iv) 693 − 811 for (iii) PCD patients and (iv) healthy subjects, respectively using hand-held analyzer MINO2.

further functional studies to delineate the complex effects that perturbation of cilia structure and function have on the Hh signaling pathway in cholangiocytes in relation to the BA phenotype, are warranted.

To conclude, our findings indicate that genetic factors have a more direct role in nonsyndromic BA pathogenesis than previously thought. The excess burden of mutations in liver expressed ciliary genes, conferring absence of cilia in some patients' bile duct, implicate that malformed cilia or reduced ciliary function in the vulnerable neonatal biliary system can lead to aberrant Hh signaling pathway. Especially when exposed to bile acids, the ciliary abnormalities may result in biliary fibrosis, inflammation, and eventually chronic liver injury. Elucidation of disease mechanisms of BA may help in the development of preventative or/and therapeutic strategies to improve the clinical outcome.

Contributors

W.Y.L. performed the genetics analyses. W.Y.L. and J.S.H contributed to bioinformatics data processing. M.T.S. prepared the samples, performed Sanger sequencing and functional studies. H.Y. generated the human cholangiocytes and performed the functional studies. P. H.Y.C., J.M.N., F.Y., C.W.D.L., D.N.N, P.A.H.N., and S.L.L. recruited the subjects, collected the samples and clinical data. H.M.M, D.J. and C. O. provided insightful comments and suggestions. W.Y.L. and C.S.M. T. wrote the manuscript and verified the genetic data. P.C.S., M.M.G. B., V.C.H.L., C.S.M.T. and P.K.H.T. designed the study and supervised the project. All authors read and approved the final version of the manuscript.

Data sharing statement

The data of this study are available within the article and in the Supplementary Information, or from the authors upon request.

Declaration of Competing Interest

The authors declare that they have no competing interests.

Acknowledgments

We extend our gratitude to all the patients and their families who participated in the study, the physicians who referred and treated the patients, and other members of our laboratories for their valuable contributions over the years. Authors thank the technical staff of the Electron Microscope Unit, Queen Mary Hospital, Hong Kong for their expert assistance in the scanning and transmission electron microscopy studies.

This work was supported by research grants from the Hong Kong General Research Fund (Grant Nos. 17107314 and 766112 to M.M.G. B., 17105119 to V.C.H.L. and 17109918 to P.K.H.T.) and Health and Medical Research Fund Commissioned Paediatric Research at Hong Kong Children's Hospital (Grant No. PR-HKU-1 to P.K.H.T.). P.H.Y.C. was supported by The University of Hong Kong Li Ka Shing Faculty of Medicine Enhanced New Staff Start-up Fund. C.S.M.T. was supported by Theme-based Research scheme (T12C-714/14-R). P.K.H.T., C.S.M.T. and W.Y.L were supported by Dr. Li Dak-Sum Research Fund.

Supplementary materials

Supplementary material associated with this article can be found in the online version at doi:10.1016/j.ebiom.2021.103530.

References

[1] Jimenez-Rivera C, Jolin-Dahel KS, Fortinsky KJ, Gozdyra P, Benchimol EI. International incidence and outcomes of biliary atresia. J Pediatr Gastroenterol Nutr 2013;56(4):344–54.
[2] Smith BM, Laberge JM, Schreiber R, Weber AM, Blanchard H. Familial biliary atresia in three siblings including twins. J Pediatr Surg 1991;26(11):1331–3.
[3] Silveira TR, Salzano FM, Howard ER, Mowat AP. Congenital structural abnormalities in biliary atresia: evidence for etiopathogenic heterogeneity and therapeutic implications. Acta Paediatr Scand 1991;80(12):1192–9.
[4] Tam PKH, Chung PHY, St Peter SD, Gayer CP, Ford HR, Tam GCH, et al. Advances in paediatric gastroenterology. Lancet North Am Ed 2017;390(10099):1072–82.
[5] Mack CL, Sokol RJ. Unraveling the pathogenesis and etiology of biliary atresia. Pediatr Res 2005;57(7):87–94.
[6] Bezerra JA, Wells RG, Mack CL, Karpen SJ, Hoofnagle JH, Doo E, et al. Biliary atresia: clinical and research challenges for the twenty-first century. Hepatology 2018;68(3):1163–73.

[7] Kilgore A, Mack CL. Update on investigations pertaining to the pathogenesis of biliary atresia. Pediatr Surg Int 2017;33(12):1233–41.
[8] Garcia-Barceló MM, Yeung MY, Miao XP, Tang CS, Cheng G, Chen G, et al. Genome-wide association study identifies a susceptibility locus for biliary atresia on 10q24.2. Hum Mol Genet 2010;19(14):2917–25.
[9] Cheng G, Tang CS, Wong EH, Cheng WW, So MT, Miao X, et al. Common genetic variants regulating ADD3 gene expression alter biliary atresia risk. J Hepatol 2013;59(6):1285–91.
[10] Cui S, Leyva–Vega M, Tsai EA, EauClaire SF, Glessner JT, Hakonarson H, et al. Evidence from human and zebrafish that GPC1 is a biliary atresia susceptibility gene. Gastroenterology 2013;144(5):1107–1115.e3.
[11] Chen Y, Gilbert MA, Grochowski CM, McEldrew D, Llewellyn J, Waisbourd-Zinman O, et al. A genome-wide association study identifies a susceptibility locus for biliary atresia on 2p16.1 within the gene EFEMP1. PLoS Genet 2018;14(8):e1007532.
[12] Ningappa M, So J, Glessner J, Ashokkumar C, Ranganathan S, Min J, et al. The role of ARF6 in biliary atresia. PLoS One 2015;10(9):e0138381.
[13] Berauer JP, Mezina AI, Okou DT, Sabo A, Muzny DM, Gibbs RA, et al. Identification of polycystic kidney disease 1 like 1 gene variants in children with biliary atresia splenic malformation syndrome. Hepatology 2019;70(3):899–910.
[14] Girard M, Panasyuk G. Genetics in biliary atresia. Curr Opin Gastroenterol 2019;35(2):73–81.
[15] H. Li Aligning sequence reads, clone sequences and assembly contigs with BWA-MEM. arXiv:13033997v1 [q-bioGN].
[16] DePristo MA, Banks E, Poplin R, Garimella KV, Maguire JR, Hartl C, et al. A framework for variation discovery and genotyping using next-generation DNA sequencing data. Nat Genet 2011:43.
[17] Purcell S, Neale B, Todd-Brown K, Thomas L, Ferreira MA, Bender D, et al. PLINK: a tool set for whole-genome association and population-based linkage analyses. Am J Hum Genet 2007;81(3):559–75.
[18] Li MX, Gui HS, Kwan JS, Bao SY, Sham PC. A comprehensive framework for prioritizing variants in exome sequencing studies of mendelian diseases. Nucleic Acids Res 2012;40.
[19] Babu RO, Lui VCH, Chen Y, Yiu RSW, Ye Y, Niu B, et al. Beta-amyloid deposition around hepatic bile ducts is a novel pathobiological and diagnostic feature of biliary atresia. J Hepatol 2020.
[20] Reimand J, Kull M, Peterson H, Hansen J, Vilo J. g:Profiler – a web-based toolset for functional profiling of gene lists from large-scale experiments. Nucleic Acids Res 2007;35(suppl_2):W193–200.
[21] van Dam TJ, Wheway G, Slaats GG, Huynen MA, Giles RH, Group SS. The syscilia gold standard (SCGSv1) of known ciliary components and its applications within a systems biology consortium. Cilia 2013;2(1):7.
[22] Carbon S, Ireland A, Mungall CJ, Shu S, Marshall B, Lewis S, et al. AmiGO: online access to ontology and annotation data. Bioinformatics 2009;25(2):288–9 (Oxford, England).
[23] Hendricks AE, Billups SC, Pike HNC, Farooqi IS, Zeggini E, Santorico SA, et al. ProxECAT: proxy external controls association test. a new case-control gene region association test using allele frequencies from public controls. PLoS Genet 2018;14(10):e1007591.
[24] Cheung ID, Bagnat M, Ma TP, Datta A, Evason K, Moore JC, et al. Regulation of intrahepatic biliary duct morphogenesis by claudin 15-like b. Dev Biol 2012;361(1):68–78.
[25] Garnaas MK, Cutting CC, Meyers A, Kelsey PB, Harris JM, North TE, et al. Rargb regulates organ laterality in a zebrafish model of right atrial isomerism. Dev Biol 2012;372(2):178–89.
[26] Schaub M, Nussbaum J, Verkade H, Ober EA, Stainier DY, Sakaguchi TF. Mutation of zebrafish snapc4 is associated with loss of the intrahepatic biliary network. Dev Biol 2012;363(1):128–37.
[27] Wilkins BJ, Gong W, Pack M. A novel keratin18 promoter that drives reporter gene expression in the intrahepatic and extrahepatic biliary system allows isolation of cell-type specific transcripts from zebrafish liver. Gene Expr Patterns 2014;14(2):62–8.
[28] Matthews RP, EauClaire SF, Mugnier M, Lorent K, Cui S, Ross MM, et al. DNA hypomethylation causes bile duct defects in zebrafish and is a distinguishing feature of infantile biliary atresia. Hepatology 2011;53(3):905–14.
[29] Schneider CA, Rasband WS, Eliceiri KW. NIH image to imageJ: 25 years of image analysis. Nat Methods 2012;9:671.
[30] Marthin JK, Nielsen KG. Hand-held tidal breathing nasal nitric oxide measurement-a promising targeted case-finding tool for the diagnosis of primary ciliary dyskinesia. PLoS One 2013;8(2):e57262.
[31] Lee SL, O'Callaghan C, Lau YL, Lee CD. Functional analysis and evaluation of respiratory cilia in healthy Chinese children. Respir Res 2020;21(1):259.
[32] Hartley JL, O'Callaghan C, Rossetti S, Consugar M, Ward CJ, Kelly DA, et al. Investigation of primary cilia in the pathogenesis of biliary atresia. J Pediatr Gastroenterol Nutr 2011;52(4):485–8.
[33] Sironen A, Kotaja N, Mulhern H, Wyatt TA, Sisson JH, Pavlik JA, et al. Loss of SPEF2 function in mice results in spermatogenesis defects and primary ciliary dyskinesia. Biol Reprod 2011;85(4):690–701.
[34] Jurczyk A, Gromley A, Redick S, Agustin JS, Witman G, Pazour GJ, et al. Pericentrin forms a complex with intraflagellar transport proteins and polycystin-2 and is required for primary cilia assembly. J Cell Biol 2004;166(5):637–43.
[35] Tobin JL, Beales PL. The nonmotile ciliopathies. Genet Med 2009;11(6):386–402.
[36] Shapiro AJ, Davis SD, Polineni D, Manion M, Rosenfeld M, Dell SD, et al. Diagnosis of primary ciliary dyskinesia. An official American thoracic society clinical practice guideline. Am J Respir Crit Care Med 2018;197(12):e24–39.
[37] Narang I, Ersu R, Wilson NM, Bush A. Nitric oxide in chronic airway inflammation in children: diagnostic use and pathophysiological significance. Thorax 2002;57(7):586–9.
[38] Walker WT, Jackson CL, Lackie PM, Hogg C, Lucas JS. Nitric oxide in primary ciliary dyskinesia. Eur Respir J 2012;40(4):1024–32.
[39] Saternos HC, AbouAlaiwi WA. Signaling interplay between primary cilia and nitric oxide: a mini review. Nitric Oxide 2018;80:108–12.
[40] Bontems F, Fish RJ, Borlat I, Lembo F, Chocu S, Chalmel F, et al. C2orf62 and TTC17 are involved in actin organization and ciliogenesis in zebrafish and human. PLoS One 2014;9(1):e86476.
[41] Nonaka S, Tanaka Y, Okada Y, Takeda S, Harada A, Kanai Y, et al. Randomization of left-right asymmetry due to loss of nodal cilia generating leftward flow of extraembryonic fluid in mice lacking KIF3B motor protein. Cell 1998;95(6):829–37.
[42] Engelke MF, Waas B, Kearns SE, Suber A, Boss A, Allen BL, et al. Acute inhibition of heterotrimeric kinesin-2 function reveals mechanisms of intraflagellar transport in mammalian cilia. Curr Biol 2019;29(7):1137–1148.e4.
[43] Omenetti A, Diehl AM. Hedgehog signaling in cholangiocytes. Curr Opin Gastroenterol 2011;27(3):268–75.
[44] Machado MV, Diehl AM. Hedgehog signaling in liver pathophysiology. J Hepatol 2018;68(3):550–62.
[45] Grzelak CA, Martelotto LG, Sigglekow ND, Patkunanathan B, Ajami K, Calabro SR, et al. The intrahepatic signaling niche of hedgehog is defined by primary cilia positive cells during chronic liver injury. J Hepatol 2014;60(1):143–51.
[46] Wong SY, Seol AD, So PL, Ermilov AN, Bichakjian CK, Epstein EH, et al. Primary cilia can both mediate and suppress hedgehog pathway–dependent tumorigenesis. Nat Med 2009;15(9):1055–61.
[47] Huangfu D, Anderson KV. Cilia and hedgehog responsiveness in the mouse. Proc Natl Acad Sci U. S. A. 2005;102(32):11325–30.
[48] Chu AS, Russo PA, Wells RG. Cholangiocyte cilia are abnormal in syndromic and non-syndromic biliary atresia. Mod Pathol 2012;25:751.
[49] Frassetto R, Parolini F, Marceddu S, Satta G, Papacciuoli V, Pinna MA, et al. Intrahepatic bile duct primary cilia in biliary atresia. Hepatol Res 2018;48(8):664–74.
[50] Karjoo S, Hand NJ, Loarca L, Russo PA, Friedman JR, Wells RG. Extrahepatic cholangiocyte cilia are abnormal in biliary atresia. J Pediatr Gastroenterol Nutr 2013;57(1):96–101.
[51] Jung HY, Jing J, Lee KB, Jang JJ. Sonic hedgehog (SHH) and glioblastoma-2 (Gli-2) expressions are associated with poor jaundice-free survival in biliary atresia. J Pediatr Surg 2015;50(3):371–6.
[52] Xu X, Zhan J. Biliary atresia in twins: a systematic review and meta-analysis. Pediatr Surg Int 2020;36(8):953–8.
[53] Tang V, Cofer ZC, Cui S, Sapp V, Loomes KM, Matthews RP. Loss of a candidate biliary atresia susceptibility gene, add3a, causes biliary developmental defects in zebrafish. J Pediatr Gastroenterol Nutr 2016;63(5):524–30.
[54] Rajagopalan R, Tsai EA, Grochowski CM, Kelly SM, Loomes KM, Spinner NB, et al. Exome sequencing in individuals with isolated biliary atresia. Sci Rep 2020;10(1):2709.